Mol Cell Biochem (2007) 301:241–249
DOI 10.1007/s11010-007-9417-6

Morphology, cytoskeletal organization, and myosin dynamics of mouse embryonic fibroblasts cultured on nanofibrillar surfaces

Ijaz Ahmed · Abdul S. Ponery · Alam Nur-E-Kamal · Jabeen Kamal · Adam S. Meshel · Michael P. Sheetz · Melvin Schindler · Sally Meiners

Received: 20 October 2006 / Accepted: 19 January 2007 / Published online: 9 February 2007

Abstract Growth of cells in tissue culture is generally performed on two-dimensional (2D) surfaces composed of polystyrene or glass. Recent work, however, has shown that such 2D cultures are incomplete and do not adequately represent the physical characteristics of native extracellular matrix (ECM)/basement membrane (BM), namely dimensionality, compliance, fibrillarity, and porosity. In the current study, a three-dimensional (3D) nanofibrillar surface composed of electrospun polyamide nanofibers was utilized to mimic the topology and physical structure of ECM/BM. Additional chemical cues were incorporated into the nanofibrillar matrix by coating the surfaces with fibronectin, collagen I, or laminin-1. Results from the current study show an enhanced response of primary mouse embryonic fibroblasts (MEFs) to culture on nanofibrillar surfaces with more dramatic changes in cell spreading and reorganization of the cytoskeleton than previously observed for established cell lines. In addition, the cells cultured on nanofibrillar and 2D surfaces exhibited differential responses to the specific ECM/BM coatings. The localization and activity of myosin II-B for MEFs cultured on nanofibers was also compared. A dynamic redistribution of myosin II-B was observed within membrane protrusions. This was previously described for cells associated with nanofibers composed of collagen I but not for cells attached to 2D surfaces coated with monomeric collagen. These results provide further evidence that nanofibrillar surfaces offer a significantly different environment for cells than 2D substrates.

Keywords Nanofibers · Nanofibrillar surfaces · Extracellular matrix · Mouse embryonic fibroblasts · Myosin II-B · Fibronectin · Laminin-1 · Collagen I

I. Ahmed · A. S. Ponery · J. Kamal · S. Meiners (✉)
Department of Pharmacology, UMDNJ-Robert Wood Johnson Medical School, 675 Hoes Lane, Piscataway, NJ 08854, USA
e-mail: meiners@umdnj.edu

A. Nur-E-Kamal
Department of Biology, Medgar-Evers College of the City University of New York, Brooklyn, NY 11225, USA

A. S. Meshel · M. P. Sheetz
Department of Biological Sciences, Columbia University, New York, NY 10027, USA

M. Schindler
NanoCulture, LLC, 117 Bedford Court, Piscataway, NJ 08854, USA

Introduction

A technical challenge for cell biologists has been the development of culture methods for anchorage dependent cells that is not only permissive for cell growth, but also promotes an in vivo repertoire of cellular activities [1–4]. Current methods of culturing anchorage dependent cells are largely dependent upon growth of cells on two- dimensional (2D) surfaces that are either modified with charged groups or coated with proteins or peptides derived from the extracellular matrix/basement membrane (ECM/BM) [4–6]. Recent studies suggest that although 2D coatings can enhance certain cellular functions, the presentation of ECM/BM proteins and alterations in their conformation within a three-dimensional (3D) matrix may be critical parameters that increase their effectiveness for promoting functional and structural changes between and within cells [7–10].

To provide a more topologically mimetic geometry and porosity of the ECM/BM for cell culture, the development of a synthetic nanofibrillar and nanoporous electrospun polyamide surface was pursued [11]. Electrospinning is a technique previously employed in filtration [12] and tissue engineering [13–15] that has been extended to cell culture applications [11, 16]. Previous work demonstrated that culture of NIH 3T3 fibroblasts and normal rat kidney (NRK) cells on polyamide nanofibrillar surfaces yielded dramatic changes in cellular morphology such that the cells more closely resembled their in vivo counterparts. These changes were reflected in the extent of cell spreading, actin organization, focal adhesion composition, clustering of integrins, fibronectin organization, and Rac activation [11, 16]. Thus, the results suggested that polyamide nanofibers provide a culture surface that may yield more physiologically relevant experimental results.

Although the observed morphological changes were striking, this work was conducted using a synthetic nanofibrillar surface that mimicked the architecture, but not the chemistry, of the ECM/BM. Clearly, another important element that must be addressed in the design of biomimetic surfaces is the incorporation and presentation of signaling cues that are contained within the sequences of the molecules comprising the ECM/BM [17–21]. Moreover, the previous experiments [11, 16] were conducted with established cell lines that had been selected over time to grow on 2D surfaces. Such cells may not be capable of reflecting phenotypic changes promoted by culture on a nanofibrillar surface to the same extent as primary cells, which have been removed from their in vivo environments. Therefore, in the current study, the hypothesis was evaluated that nanofibrillar surfaces composed of polyamide nanofibers, alone or coated with ECM/BM proteins, can recreate a more in vivo-like environment for primary cells. The hypothesis that nanofibrillar surfaces can differentially effect regulation of cellular activities such as myosin II-B dynamics was also explored.

Materials and methods

Reagents

The reagents and dilutions employed in this study were as follows. Fibronectin, collagen I, laminin-1, monoclonal α-actinin antibody, and monoclonal vinculin antibody were obtained from Sigma Chemical Co. (St. Louis, MO). Phalloidin-Alexa Fluor 488 was obtained from Molecular Probes (Eugene, OR). CY3-goat anti-mouse IgG (H + L) and normal goat serum were from Jackson Labs (West Grove, PA). GelMount (aqueous mounting medium with anti-fading agents) was obtained from Biomedia (Foster City, CA). Dulbecco's Modified Eagle's Medium (DMEM) (high glucose), calf serum, and fetal calf serum were all obtained from Invitrogen (Carlsbad, CA). Cell culture plates were purchased from Corning (Corning, NY).

Nanofiber production by electrospinning

Coverslips coated with electrospun polyamide nanofibers (Ultra-Web™ Synthetic ECM), actually a continuous fiber that collects as a nonwoven fabric, were obtained from Donaldson Co., Inc. (Minneapolis, MN, USA) (www.synthetic-ecm.com). The nanofibers were electrospun onto plastic coverslips in a controlled thickness (2 μm) and fiber density from a blend of two polymers $(C_{28}O_4N_4H_{47})_n$ and $(C_{27}O_{4.4}N_4H_{50})_n$. The polymeric nanofiber mat was then crosslinked in the presence of an acid catalyst.

Measurements of the adsorption of fibronectin, collagen I, and laminin-1

Extracellular matrix proteins (fibronectin, collagen I, and laminin-1) were dissolved in Hank's buffered saline solution (HBSS) at a final concentration of 10 μg/ml. First, the fibronectin solution (500 μl) was added to 6 polystyrene coverslips, 6 plastic (Aclar) coverslips, and 6 pieces of flat polyamide film (the same size as the coverslips (18 mm)) placed into 12 well plates. After overnight incubation at 37°C, coverslips were washed (3×) with HBSS. Adsorbed proteins were eluted with SDS Laemmli sample buffer (100 μl) and incubated at 95°C for 5 min. Two sequential extractions were performed on the same disks. Next, all 3 protein solutions (500 μl) were added to 6 nanofiber-coated Aclar and 6 uncoated Aclar coverslips placed into 12 well plates, incubated overnight, and extracted as above.

Aliquots (10 μl) were spotted onto a nitrocellulose membrane (Bio-Rad, Hercules, CA) and air-dried for 1 h. The membrane was washed (3×) with distilled water and treated with the corresponding antibodies against fibronectin, (1:1000), laminin-1 (1:1000), or collagen I (1:500) in 2% skim milk in Tris-Buffered Saline Tween-20 (TBST) at 4°C for 18 h. Membranes were washed (3×) with TBST. Membranes were treated with a horseradish peroxidase-conjugated secondary antibody and developed using an enhanced chemiluminescence (ECL) kit purchased from Pierce

(Rockford, IL). Spots were imaged using a Kodak Imaging Station 2000R and quantitated using the manufacturer's analytical programs.

Cell culture and fluorescence staining

MEFs were prepared from 14-day embryos derived from pregnant Swiss mice. Briefly, embryos were decapitated, eviscerated, rinsed with HBSS, minced with a razor blade, and incubated at 37°C in 0.05% trypsin/EDTA solution for 15 min with intermittent shaking. The cells were dissociated by vigorous pipetting with a fine bore fire-polished glass pipette and filtered through a 100 μm nylon mesh. The dissociated cells were centrifuged in DMEM (4.5 g/l glucose) supplemented with 10% bovine calf serum and penicillin/streptomycin. Cells obtained from 2 embryos were plated onto a 150 mm cell culture dish. After 3 days, the cells were split at a ratio of 1:3. Cells from the third passage were used for the experiments described in this study. MEFs were seeded at 1.25×10^4 cells/well in 24 well tissue culture plates and cultured in DMEM (4.5 g/l glucose) in the presence of 10% calf serum at 5% CO_2 and 37°C. Cells were grown on either 12 mm Aclar or nanofiber-coated Aclar coverslips, or on Aclar or nanofiber-coated Aclar coverslips with adsorbed fibronectin, collagen I, or laminin-1.

To adsorb the ECM/BM proteins, the coverslips or nanofiber-coated coverslips were incubated with fibronectin, collagen I, or laminin-1 (10 μg/ml) in HBSS for 18 h at 37°C. Excess protein was then washed away with HBSS (3×) and cells were plated. Under all culture conditions employed in this study, nanofibers were exposed to 10% serum proteins after being coated with a particular ECM/BM protein. Nanofibers coated with 10% serum proteins were utilized as controls.

Staining for F-actin was performed in the following manner. Cells were rinsed once with phosphate buffered saline (PBS), fixed with 4% paraformaldehyde in PBS (15 min), washed with PBS, treated with 0.5% Triton X-100 (5 min), washed with PBS, incubated with phalloidin-Alexa Fluor 488 (diluted 1:100 with PBS containing 0.3% Triton-X-100) for 1 h, washed with PBS (3×, 5min per wash), and then mounted on a slide with GelMount. Mouse monoclonal antibody staining was performed as described for phalloidin-Alexa Fluor 488 staining except after the treatment with Triton X-100, cells were washed with PBS, blocked with normal goat serum (diluted with PBS/0.3% Tween-20) for 30 min at room temperature, washed with PBS (3×, 5 min per wash), incubated overnight with primary antibody, washed with PBS (3×, 5 min per wash) followed by incubation for 1 h with the secondary antibody goat anti-mouse IgG*CY3 (diluted with PBS/0.3% Tween-20), washed with PBS (3×, 5 min per wash), and then mounted on a slide with Gel-Mount. Imaging was performed with a Zeiss Axioplan Epi-Fluorescent Microscope. Routine controls were performed for staining.

Morphometry measurements

Measurements of projected cell area were performed utilizing the software routines in the NIH Image J package (W. Rasband; NIH, Bethseda, MD; http://rsb.info.nih.gov/ImageJ). Cells (50–60 per sample) were measured employing a random sampling method.

Measurement of myosin II-B activity

Analysis of myosin II-B movement and localization were performed utilizing digital image fluorescence microscopy of a GFP-myosin II-B construct transfected into MEFs as described [22].

Statistical analyses of protein adsorption and cellular area

All values are given as the mean ± the standard error of the mean. The Student's *t*-test was used to compare the means. A value of $P < 0.05$ was taken as significant.

Results

Adsorption of fibronectin to 2D surfaces composed of Aclar, polystyrene, and polyamide

As observed in Fig. 1, both Aclar and polystyrene adsorbed fibronectin significantly better than a two-dimensional surface composed of polyamide. No protein was detected in the second extraction on the 2D polyamide surface, suggesting proteins do not adhere well to this formulation of polyamide. Moreover, cellular adherence to 2D polyamide surfaces was not detected (data not shown).

Adsorption of fibronectin, collagen I, and laminin-1 to nanofibrillar and 2D surfaces

As shown in Fig. 2, the ratio of protein adsorbed to nanofibrillar surfaces normalized to the amount adsorbed to Aclar surfaces demonstrates that higher levels of collagen I, laminin-1, and fibronectin bound to

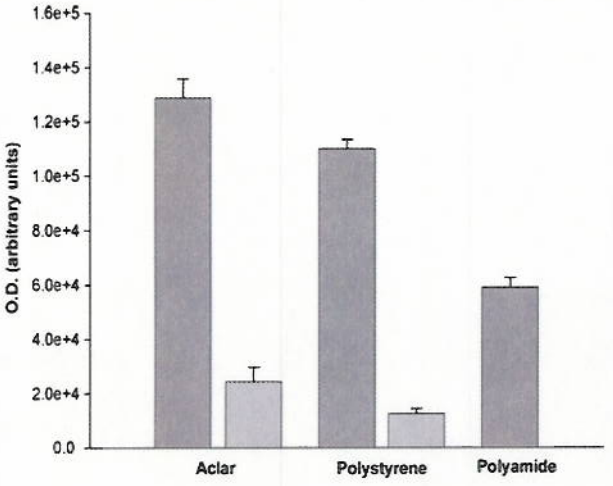

Fig. 1 Adsorption of fibronectin to 2D surfaces composed of Aclar, polystyrene, or polyamide. Dark gray bars represent the first extraction of fibronectin, while light gray bars represent the second extraction. Protein adsorption is given in arbitrary units of absorption. Data are shown as the mean ± the standard error ($n = 6$). The first extraction from Aclar and polystyrene was significantly greater than the second ($P < 0.001$), whereas no protein was detected in the second extraction from polyamide

nanofibrillar surfaces than to Aclar. The amounts varied between ~3- (laminin-1) to 7.5- (fibronectin) fold higher. How much of this extra protein is actually sensed by the cells remains to be determined.

Actin organization in MEFs cultured on nanofibrillar and 2D surfaces

MEFs cultured on nanofibrillar surfaces and stained for F-actin (Fig. 3B) exhibited a striking difference in cell spreading and actin organization in comparison to MEFs cultured on a 2D Aclar coverslip (Fig. 3A). The former had a smaller projected area and tended to have a more elongated morphology. The number at the bottom left corner of each image is the percentage of cells displaying stress fibers. While 94% of the cells cultured on the 2D surface displayed a significant number of stress fibers, cells cultured on nanofibrillar surfaces displayed few or no stress fibers. Approximately 80% of the MEFs cultured on nanofibers demonstrated punctate actin patches (Fig. 3B), whereas punctate actin patches were not observed for well spread cells cultured on the more adherent 2D plastic surfaces (Fig. 3A). Therefore, in terms of cell shape and membrane ruffling (evidenced by actin patches), the nanofibrillar matrix promoted a morphology for MEFs that was reminiscent of an in vivo migratory phenotype.

Cells were then cultured on surfaces coated with ECM proteins. The percentage of cells with a significant number of stress fibers that were cultured on 2D surfaces coated with fibronectin (Fig. 3C) or collagen I (Fig. 3E) was similar to the percentage of cells with stress fibers that were cultured on the uncoated 2D surface not coated with these proteins. (~90% of the cells had stress fibers on fibronectin-coated plastic, in comparison to 80% on collagen I-coated plastic and 94% on plastic not coated with the ECM/BM proteins). In contrast, there was a large decrease in the number of cells showing stress fibers for culture on fibronectin (Fig. 3D), collagen I (Fig. 3F), and laminin-1-coated nanofibrillar surfaces (Fig. 3H). The percentage of cells with stress fibers cultured on fibronectin- or

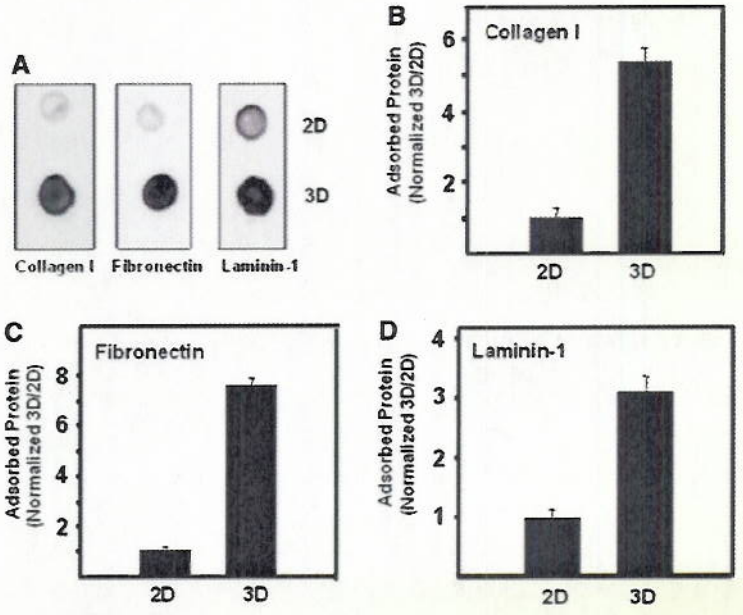

Fig. 2 Adsorption of collagen I, fibronectin, and laminin-1 onto nanofibrillar and 2D surfaces. Dot blots (**A**) were utilized to quantitate the amount of collagen I (**B**), fibronectin (**C**), and laminin-1 (**D**) adsorbed to nanofibrillar (NF) and Aclar (2D) surfaces. The first extraction is shown. Protein adsorption is given as a normalized ratio between nanofibrillar (NF) and 2D adsorption. Data are shown as the mean ± the standard error ($n = 6$). Significantly more of each protein adsorbed to the nanofibrillar surface than to Aclar ($P < 0.001$)

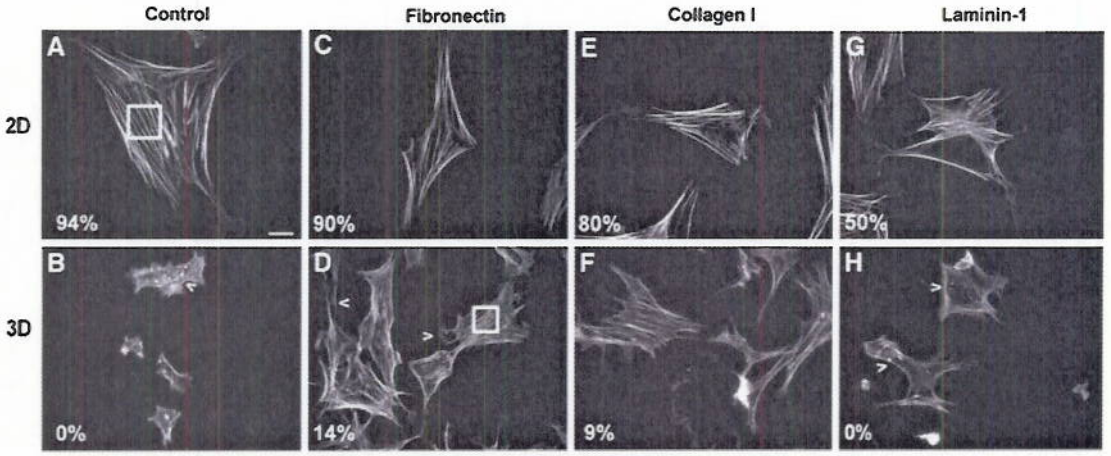

Fig. 3 F-actin organization in MEFs cultured on 2D and nanofibrillar surfaces. Panels **A**, **C**, **E**, **G** are MEFs cultured on 2D Aclar surfaces coated with fibronectin, collagen I, and laminin-1, respectively while panels **B**, **D**, **F**, **H** are MEFs cultured on nanofibrillar surfaces and nanofibrillar surfaces coated with fibronectin, collagen I, and laminin-1, respectively. Numbers in the lower left corner of panels represents the percentage of cells containing stress fibers. The boxed area in 3**A** shows stress fibers while the boxed area in 3**D** shows a parallel array of thinner F-actin fibers. Arrow-heads in 3**D** and 3**H** show dendritic extensions. Bar, 20 μm. The micrographs shown here are typical of 6 such experiments

collagen I-coated nanofibers (~14% and ~9%, respectively) (Fig. 3D, F) was slightly higher than the percentage of cells with stress fibers that were cultured on the control without ECM/BM proteins (0%) (Fig. 3B) or laminin-1-coated nanofibers (0%) (Fig. 3H). These results suggest that ECM/BM molecules when presented on nanofibrillar surfaces do not promote the formation of stress fibers to the extent normally observed when ECM/BM molecules are presented on 2D surfaces.

Although few stress fibers were observed for cells cultured on nanofibrillar surfaces, the cells cultured on fibronectin- (Fig. 3D) and collagen I-coated 3D surfaces (Fig. 3F) showed an abundance of aligned, slender F-actin containing fibrils. Moreover, unlike the cells cultured on nanofibrillar surfaces without a coating of ECM/BM proteins (Fig. 3B), MEFs did not contain punctate actin structures when cultured on fibronectin- (Fig. 3D) or collagen I- (Fig. 3F) coated nanofibers. Correspondingly, the cells also were better spread on fibronectin- (Fig. 3D) and collagen I-coated (Fig. 3F) nanofibrillar surfaces as opposed to nanofibrillar surfaces without adsorbed ECM/BM proteins (Fig. 3B). An additional feature frequently observed for MEFs cultured on fibronectin- and collagen I-coated nanofibrillar surfaces was the large number of dendritic extensions and membrane protrusions emanating from the cell body (See arrow-heads in Fig. 3D). These were far more prevalent than for MEFs cultured on fibronectin- and collagen I- coated 2D surfaces (Fig. 3C, E).

MEFs cultured on laminin-1-coated 2D (Fig. 3G) and nanofibrillar surfaces (Fig. 3H) demonstrated a population of cells with significantly fewer stress fibers than did MEFs cultured on fibronectin- (Fig. 3C) or collagen I- (Fig. 3E) coated 2D surfaces. Approximately 50% of the cells had stress fibers on the laminin-1-coated 2D surface (Fig. 3G), and none of the cells had stress fibers on the laminin-1-coated nanofibrillar surfaces (Fig. 3H). The cells cultured on the laminin-1-coated nanofibrillar surfaces (Fig. 3H) also contained a population of thin F-actin fibrils that were more diffuse than those observed for cells cultured on fibronectin- (Fig. 3D) or collagen I- (Fig. 3F) coated nanofibrillar surfaces. In addition, a considerable number of cells (~35% of the population) contained punctate patches of F-actin, which were not observed for cells cultured on the laminin-1-coated 2D surface (Fig. 3G).

Vinculin localization in MEFs cultured on nanofibrillar and 2D surfaces

Vinculin is a prominent component of the focal complexes and focal adhesions [23–25] that link the cytoskeleton, plasma membrane, and ECM. As shown in Fig. 4A, vinculin had the characteristic streaked appearance described for its association with focal adhesions formed on 2D surfaces [24, 25]. In contrast, culture of MEFs on uncoated nanofibrillar surfaces resulted in the localization of vinculin to punctate structures that were predominantly found on the dorsal

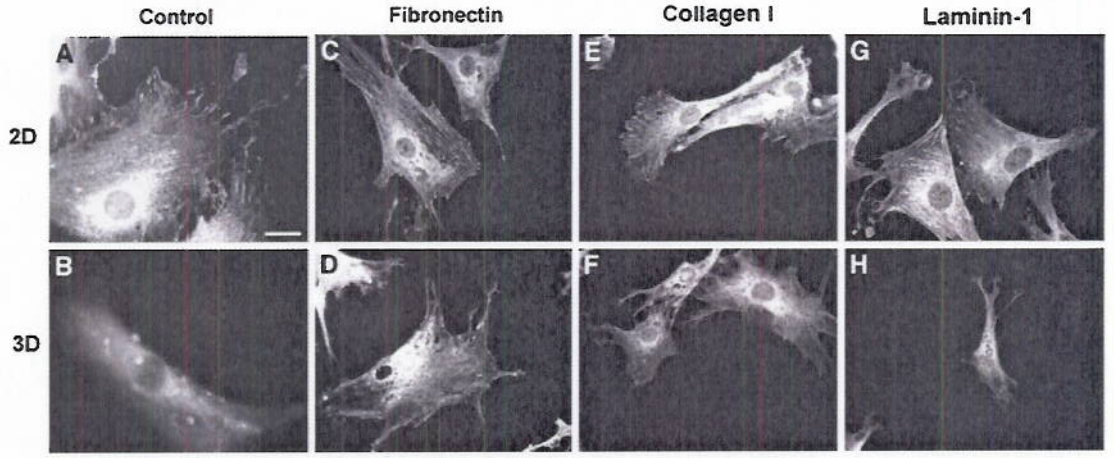

Fig. 4 Vinculin organization in MEFs cultured on nanofibrillar and 2D surfaces. Panels **A**, **C**, **E**, **G** are MEFs cultured on 2D Aclar surfaces and Aclar coated with fibronectin, collagen I, and laminin-1, respectively; while panels **B**, **D**, **F**, **H** depict MEFs cultured on nanofibrillar surfaces and nanofibrillar surfaces coated with fibronectin, collagen I, and laminin-1. Bar, 20 μm. The micrographs shown here are typical of 6 such experiments

membrane surface (Fig. 4B; microscope focused to the dorsal surface of the cell).

MEFs cultured on fibronectin- (Fig. 4C) or collagen I- (Fig. 4E) coated 2D surfaces also showed the "classic" pattern observed for vinculin staining in focal adhesions (Fig. 4C, E), while MEFs cultured on fibronectin- (Fig. 4D) or collagen I- (Fig. 4F) coated nanofibrillar surfaces showed significantly fewer patches of vinculin staining, indicative of a loss of focal adhesions. Cells cultured on laminin-1-coated 2D surfaces (Fig. 4G) showed less distinct vinculin staining than was observed for cells cultured on fibronectin- (Fig. 4C) or collagen I- (Fig. 4E) coated 2D surfaces. Cells cultured on laminin-1-coated nanofibrillar surfaces (Fig. 4H) had weakly staining fibrils with a few intense patches of vinculin staining, again demonstrating that laminin-1 does not alter nanofibrillar properties in terms of fibroblast phenotype to the same extent as fibronectin and collagen I.

α-actinin localization in MEFs cultured on nanofibrillar and 2D surfaces

α-actinin is an important linker protein that is required for the formation of F-actin bundles and helps to connect F-actin fibrils to integrins in the cell membrane [26]. As observed in Fig. 5, MEFs stained for α-actinin revealed a pattern of fibrillar staining that was the most pronounced for cells cultured on the 2D control without a coating of ECM/BM proteins (Fig. 5A) and on 2D surfaces coated with fibronectin (Fig. 5C) or collagen I (Fig. 5E). α-actinin staining for cells cultured on the laminin-1-coated 2D surface (Fig. 5G), as was observed for stress fibers, demonstrated some cells with α-actinin fibrils and some without prominent staining. Hence α-actinin staining mirrored the fibrillar pattern of F-actin staining observed in Fig. 3.

Projected surface area of MEFs cultured on nanofibrillar and 2D surfaces

MEFs are a heterogenous population with a range of cell shapes and sizes. However, quantification of the mean surface area did reveal significant trends. For example, a dramatic change in the surface area was revealed for cells cultured on nanofibrillar versus 2D surfaces without a coating of ECM/BM proteins (Fig. 6), with much smaller cells on the nanofibrillar surface. Coating the 2D surfaces with fibronectin, collagen I, or laminin-1 resulted in a marked decrease in the surface area for MEFs in comparison to that observed on 2D surfaces without a coating of ECM/BM proteins. On the other hand, coating the 3D nanofibrillar surfaces with fibronectin or collagen I resulted in a larger MEF projected surface area, whereas laminin-1 had little effect.

Distribution of myosin II-B in MEFs cultured on nanofibrillar and 2D surfaces

The ability of MEFs to extend membrane protrusions on nanofibers was next examined. MEFs transfected with GFP-myosin-II-B were imaged after 3 h of culture using time-lapse digital image microscopy [22]. As shown in Fig. 7, GFP-myosin II-B relocated within peripheral protrusions that extended and contracted (see arrows in sequences).

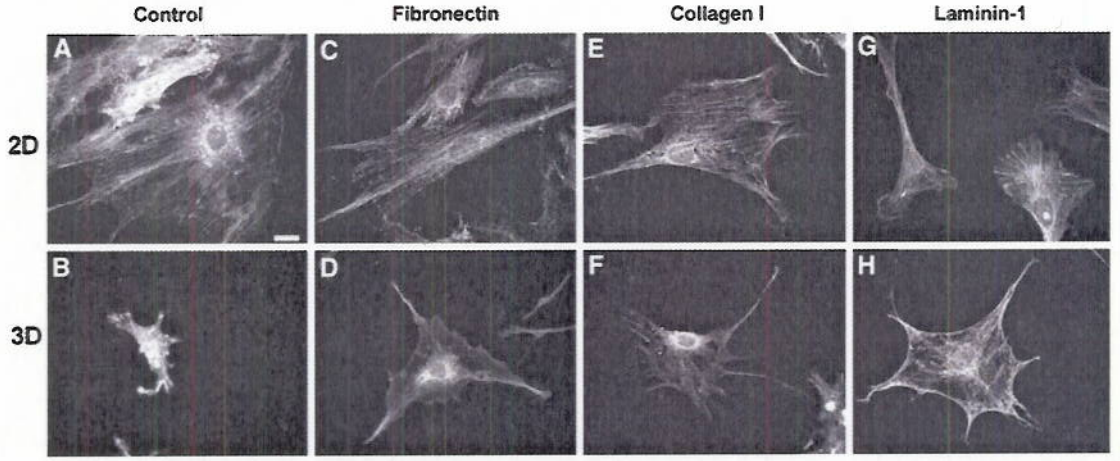

Fig. 5 α-actinin organization in MEFs cultured on 2D Aclar and 3D nanofibrillar surfaces. Panels **A**, **C**, **E**, **G** are MEFs cultured on Aclar and Aclar coated with fibronectin, collagen I, and laminin-1, respectively; while panels **B**, **D**, **F**, **H** are MEFs cultured on nanofibrillar surfaces and nanofibrillar surfaces coated with fibronectin, collagen I, and laminin-1. Bar, 20 μm. The micrographs shown here are typical of 6 such experiments

Discussion

In one of the first studies to address the discrepancy between in vitro and in vivo cellular architecture, Cukierman et al. [7] demonstrated that, in addition to the molecular complexity of the ECM, two physical parameters are important for ECM-mediated cell organization: the three-dimensionality and the rigidity (or compliance) of the ECM. The investigators observed that cells demonstrated significant differences in migration, proliferation rate, and the structure and composition of focal adhesions when cultured on compliant cell-free 3D ECM matrices derived from mouse embryos. Evidence was provided that these differences more accurately mimicked in vivo cellular organization.

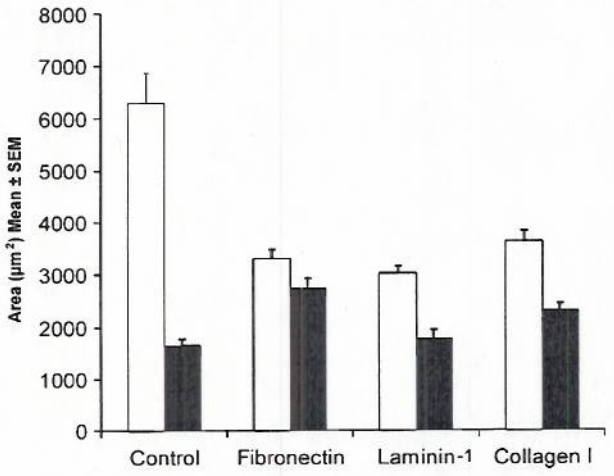

Fig. 6 Analysis of the projected spread area of cells adhering to nanofibrillar and 2D Aclar surfaces coated with fibronectin, collagen I, and laminin-1. Unfilled and filled bars represent spread area of cells on Aclar and nanofibrillar surfaces, respectively. Data are shown as mean ± standard error ($n = 3$). Cellular areas on Aclar were significantly greater than cellular areas on the nanofibrillar surface in each case ($P < 0.001$ for control, laminin-1, and collagen-1; $P < 0.05$ for fibronectin)

In a previous report [11], we demonstrated that many structural consequences of culturing cells on animal-derived 3D matrices could be recapitulated by culturing immortalized cells on matrices composed of interconnected highly porous networks of nanofibers. The current report extends these observations to primary fibroblasts and further evaluates the impact of incorporating ECM/BM molecules onto the nanofibrillar surface. Culture of primary MEFs on fibronectin (Fig. 3D) and collagen I- (Fig. 3F) coated 3D surfaces resulted in almost a complete loss of stress fibers when compared to culture of MEFs on similarly coated 2D surfaces (Fig. 3C and 3E, respectively). The loss of stress fibers on the coated 3D surfaces was replaced by an abundance of thin actin fibrils that aligned themselves along the long axis of the cell enforcing an apical-ventral symmetry normally observed for fibroblasts in vivo. This switch in the organization of the actin cytoskeleton (Fig. 3), the change in number and organization of focal adhesions (assessed using vinculin staining) (Fig. 4), and the preferential and sustained activation of Rac [16] apparently represent a change in cytoskeletal signaling as a consequence of attachment to nanofibrillar surfaces. The differences in cell spreading and actin and vinculin organization were more pronounced than that reported for NIH 3T3 or NRK cells [11], suggesting that primary cells have a

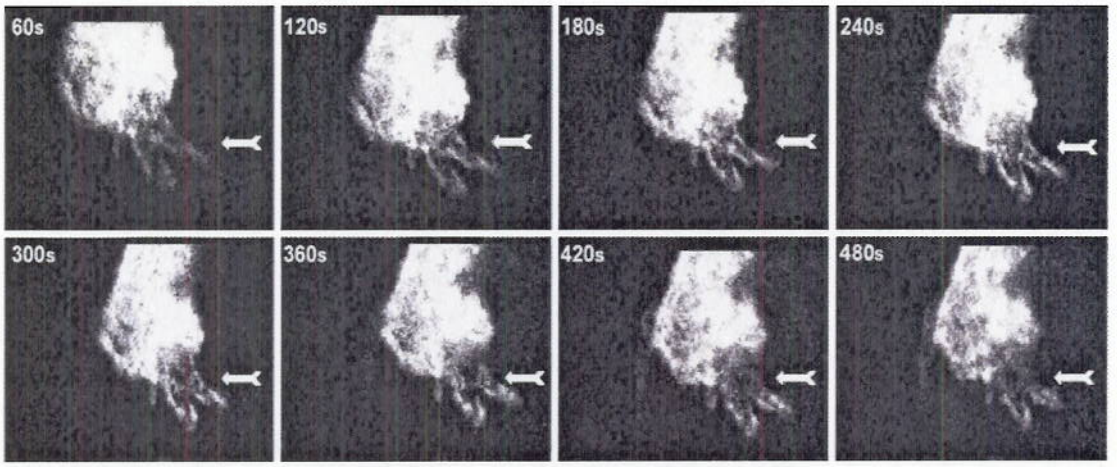

Fig. 7 Myosin II-B dynamics in membrane protrusions of cells cultured on nanofibrillar surfaces. The arrow points to the movement of myosin II-B into an extension followed by its movement out of the extension with concomitant contraction. Numbers in the upper left-hand corner are in seconds. The results shown here are typical of 3 such experiments

greater range of response to changes in surface properties than established cell lines.

Work by Watanabe et al. [27] demonstrated that expression of a constitutively active mDia1 signaling pathway resulted in the formation of thin actin fibers aligned with the long axis of the spindle-shaped cells cultured on 2D tissue culture surfaces. This was ascribed to coordinated interplay between ROCK and mDia1 segments of the Rho signaling pathway that regulated the thickness of the actin fibrils and the size and distribution of focal adhesions. We propose that a similar shift in the balance between the ROCK and mDia1 pathways is promoted by attachment to nanofibrillar surfaces leading to Rac activation [16], and the observed changes in morphology and actin/focal adhesion organization [11].

The differences in morphology and membrane ruffling observed for MEFs on nanofibrillar surfaces suggested that the dynamics of membrane protrusion and retraction would be different for cells adhering to nanofibrillar versus 2D surfaces. Meshel et al. [22] demonstrated that cells contacting collagen nanofibers on their dorsal surfaces attached to and pulled them rearward in a "hand over hand" fashion. This type of cell response was dependent on the 3D curvature of the collagen nanofiber and its interaction with $\alpha_2\beta_1$ integrins. MEFs cultured on nanofibrillar surfaces demonstrated the same type of myosin II-B dependent membrane dynamics (Fig. 7) observed for collagen nanofibers, suggesting that cells may have a common mechanical response uniquely related to 3D cues. The idea that geometry and possibly curvature are important for the observed effects of cell culture on nanofibers is further supported by work of Elliott et al. [28] in which smooth muscle cells are cultured on nanofibers (150–250 nm in diameter) composed of collagen. Changes in morphology and actin cytoskeleton organization are described, that are similar to those reported by us for culture of fibroblasts on polyamide nanofibers [11]. The results shown in Fig. 7, however, do not address the actual translocation of the collagen nanofibers described in Meshel et al. [22] and the longer time period for the extension and retraction cycles for which collagen-mediated signaling may be necessary through integrin-dependent adhesion. Significantly, as noted above, culture of NIH 3T3 and NRK cells [16] and MEFs (data not shown) on polyamide nanofibers resulted in the preferential activation of Rac and minimal activation of Rho and Cdc42. Whether the myosin II-B containing protrusions observed as MEFs pulling collagen nanofibers also occurs concomitant with similar Rac dependent mechanisms observed for 2D protrusions remains to be determined.

Why do nanofibrillar surfaces produce these differences in cell structure and signaling? As described in Cukierman et al. [9], cells in culture secrete and assemble a fibronectin-containing scaffolding or meshwork that promotes cell adherence to it rather than to the rigid surface of the tissue culture plate. This change in cell adherence is marked by a change in cell morphology and attachment with the appearance of a new type of adhesive structure, the 3D matrix adhesion [9]. In work described in Beningo et al. [29], application of a polyacrylamide gel containing fibronectin to the dorsal surface of cells resulted in a rearrangement of the cell and its actin based cytoskeleton to resemble a more in vivo-like morphology. Both studies suggest that adhesion to a 3D matrix composed of fibronectin

on the dorsal surface of the cell can release the cell from a 2D phenotype imposed by attachment to the rigid 2D surface of a tissue culture plate. This release in turn allows the cell to acquire a more in vivo-like architecture.

In our previous publications, NIH 3T3 fibroblasts and normal rat kidney cells cultured on nanofibrillar surfaces demonstrated secretion and assembly of fibronectin initially different from that observed for culture on 2D surfaces [11, 16]. As early as 6 hours, fibronectin was deposited as an extensive scaffolding on the dorsal surface of cells attached to nanofibers. This type of fibronectin-containing scaffolding is normally observed only after 2–3 days for cells cultured on 2D surfaces. We propose that culture of cells on nanofibrillar surfaces is permissive for the secretion and assembly of a 3D fibronectin containing scaffolding whose composition, spatial organization, mechanics, and signaling properties are more representative of the in vivo environment. Coating nanofibrillar surfaces with ECM/BM proteins may enhance this matrix formation and regulate its composition.

Acknowledgements This work is dedicated to the memory of Roger Keith Meiners. This work was supported by National Institutes of Health Grant R01 NS40394 and New Jersey Commission on Spinal Cord Research Grants 04–3034 SCR-E-O and 06A-007-SCR1 to S.M, and by funds from Donaldson Co., Inc.

References

1. Kim BS, Nikolovski J, Bonadio J, Smiley E, Mooney DJ (1999) Engineered smooth muscle tissues: regulating cell phenotype with the scaffold. Exp Cell Res 251:318–328
2. Sakiyama SE, Schense JC, Hubbell JA (1999) Incorporation of heparin-binding peptides into fibrin gels enhances neurite extension: an example of designer matrices in tissue engineering. FASEB J 13:2214–2224
3. Lutolf MP, Lauer-Fields JL, Schmoekel HG, Metters AT, Weber FE, Fields GB, Hubbell JA (2003) Synthetic matrix metalloproteinase-sensitive hydrogels for the conduction of tissue regeneration: engineering cell-invasion characteristics. Proc Natl Acad Sci USA 100:5413–5418
4. Schmeichel KL, Bissell MJ (2003) Modeling tissue-specific signaling and organ function in three dimensions. J Cell Sci 116:2377–2388
5. Meiners S, Mercado ML (2003) Functional peptide sequences derived from extracellular matrix glycoproteins and their receptors: strategies to improve neuronal regeneration. Mol Neurobiol 27:177–196
6. Shin H, Jo S, Mikos AG (2003) Biomimetic materials for tissue engineering. Biomaterials 24:4353–4364
7. Cukierman E, Pankov R, Stevens DR, Yamada KM (2001) Taking cell-matrix adhesions to the third dimension. Science 294:1708–1712
8. Grinnell F, Ho CH, Tamariz E, Lee DJ, Skuta G (2003) Dendritic fibroblasts in three-dimensional collagen matrices. Mol Biol Cell 14:384–395
9. Cukierman E, Pankov R, Yamada KM (2002) Cell interactions with three-dimensional matrices. Curr Opin Cell Biol 14:633–639
10. Wozniak MA, Desai R, Solski PA, Der CJ, Keely PJ (2003) ROCK-generated contractility regulates breast epithelial cell differentiation in response to the physical properties of a three-dimensional collagen matrix. J Cell Biol 163:583–595
11. Schindler M, Ahmed I, Nur-E-Kamal A, Kamal J, Grafe TH, Chung HY, Meiners S (2005) Synthetic nanofibrillar matrix promotes in vivo-like organization and morphogenesis for cells in culture. Biomaterials 26:5624–5631
12. Chung HY, Hal JRB, Gogins MA, Crofoot DG, Weik TM (2004) Polymer, polymer microfiber, polymer nanofiber and applications including filter structures. US Patent No 6,743,273 B2
13. Li WJ, Danielson KG, Alexander PG, Tuan RS (2003) Biological response of chondrocytes cultured in three-dimensional nanofibrous poly(epsilon-caprolactone) scaffolds. J Biomed Mater Res 67A:1105–1114
14. Yoshimoto H, Shin YM, Terai H, Vacanti JP (2003) A biodegradable nanofiber scaffold by electrospinning and its potential for bone tissue engineering. Biomaterials 12:2077–2082
15. Boland ED, Matthews JA, Pawlowski KJ, Simpson DG, Wnek GE, Bowlin GL. Electrospinning collagen, elastin (2004) preliminary vascular tissue engineering. Front Biosci 9:1422–1432
16. Nur-E-Kamal A, Ahmed I, Kamal J, Schindler M, Meiners S (2005) Three dimensional nanofibrillar surfaces induce activation of Rac. Biochem Biophys Res Com 331:428–434
17. Ashkenas J, Muschler J, Bissell MJ (1996) The extracellular matrix in epithelial biology: shared molecules and common themes in distant phyla. Dev Biol 180:433–444
18. Kalluri R. (2003) Basement membranes: structure, assembly and role in tumour angiogenesis. Nat Rev Cancer 3:422–433
19. Kleinman HK, Philp D, Hoffman MP (2003) Role of the extracellular matrix in morphogenesis. Curr Op Biotech 14:526–532
20. Katz BZ, Zamir E, Bershadsky A, Kam Z, Yamada KM, Geiger B (2000) Physical state of the extracellular matrix regulates the structure and molecular composition of cell-matrix adhesions. Mol Biol Cell 11:1047–1060
21. Hynes RO (1999) The dynamic dialogue between cells and matrices: implications of fibronectin's elasticity. Proc Natl Acad Sci USA 96:2588–2590
22. Meshel AS, Wei Q, Adelstein R, Sheetz MP (2005) Basic mechanism of three-dimensional collagen fibre transport by fibroblasts. Nat Cell Biol 7:157–164
23. Geiger B, Bershadsky A, Pankov R, Yamada KM (2001) Transmembrane cross-talk between the extracellular matrix-cytoskeleton. Nature Rev Mol Cell Biol 2:793–805
24. Zamir E, Geiger B (2001) Molecular complexity and dynamics of cell-matrix adhesions. J Cell Sci 14:3583–3590
25. Craig SW, Chen H (2003) Lamellipodia protrusion: moving interations of vinculin and Arp2/3. Curr Biol 13:R236–238
26. Djinović-Carugo K, Young P, Gautel M, Saraste M (1999) Structure of the α-actinin rod: molecular basis for cross-linking of actin filaments. Cell 98:537–546
27. Watanabe N, Kato T, Fujita A, Ishizaki T, Narumiya S (1999) Cooperation between mDia1 and ROCK in rho-induced actin reorganization. Nature Cell Biol 1:136–143
28. Elliott JT, Woodward JT, Langenbach KJ, Tona A, Jones PL, Plant AL (2005) Vascular smooth muscle cell response on thin films of collagen. Matrix Biol 7:489–502
29. Beningo KA, Dembo M, Wang Y-L (2004) Responses of fibroblasts to anchorage of dorsal extracellular matrix receptors. Proc Natl Acad Sci USA 101:18024–18029